has been shown in the previous study[7]: the heat transfer results are insensitive to the layer structure of the system, which, of course, has contradicted the results obtained here.

Despite its insufficiency to resolve the layer structures, the effective permeability model has been used widely in engineering design for its simplicity. Thus, there is a compelling need to evaluate the applicable range of the model. To this end, heat transfer results for the case of $k_1/k_2 = 1$ are plotted in Fig. 3 where the Rayleigh numbers are based on the effective permeability defined in Eqs. (9) and (10), respectively. While the symbols represent the results obtained from the layer model, the solid line is the result using an effective permeability. It is clear that the effective permeability model using harmonic means, although unable to reveal the characteristics of a layered structure, has a better agreement in the predicted heat transfer results. The model based on the arithmetic mean, on the other hand, considerably overestimates the heat transfer results. However, it should be noticed that, as the permeability contrast sharpens (particularly for $K_1/K_2 >> 1$), even the harmonic mean model cannot predict the heat transfer results accurately.

Conclusions

Natural convection in horizontal-layered porous annuli has been numerically investigated. The applicability of the effective permeability model in the calculation of heat transfer results of a nonuniform system has also been examined. From the present results, it is found that the normalized Nusselt number of a layered annulus with $K_1/K_2 < 1$ is always greater than that of a homogeneous one, whereas it is constantly less for an annulus with $K_1/K_2 > 1$. It is also found that the heat transfer prediction using a harmonic average permeability usually gives a better result than that of using an arithmetic average. However, as the permeability contrast increases ($K_1/K_2 >> 1$), the harmonic mean permeability model also fails. The results thus obtained are useful in the design of insulation systems and nuclear waste repositories. Although each application may have a different emphasis (e.g., minimal heat loss for pipe insulation and least contamination for waste disposal), the present results suggest that, by a careful matching of the sublayer materials, most requirements can be met easily.

Acknowledgment

The authors gratefully acknowledge the partial support received from the Department of Energy. Valuable suggestion from M. Yovanovich of University of Waterloo, is also gratefully acknowledged.

References

[1]Masuoka, T., Katsuhara, T., Nakazono, Y., and Isozaki, S., "Onset of Convection and Flow Patterns in a Porous Layer of Two Different Media," *Heat Transfer: Japanese Research*, Vol. 7, 1978, pp. 39–52.

[2]Rana, R., Horne, R. N., and Cheng, P., "Natural Convection in a Multi-Layered Geothermal Reservoir," *Journal of Heat Transfer*, Vol. 101, No. 3, 1979, pp. 411–416.

[3]McKibbin, R., and O'Sullivan, M. J., "Onset of Convection in a Layered Porous Medium Heated from Below," *Journal of Fluid Mechanics*, Vol. 96, 1980, pp. 375–393.

[4]McKibbin, R., and O'Sullivan, M. J., "Heat Transfer in a Layered Porous Medium Heated from Below," *Journal of Fluid Mechanics*, Vol. 111, 1981, pp. 141–173.

[5]Poulikakos, D., and Bejan, A., "Natural Convection in Vertically and Horizontally Layered Porous Media Heated from the Side," *International Journal of Heat and Mass Transfer*, Vol. 26, No. 12, 1983, pp. 1805–1814.

[6]Lai, F. C., and Kulacki, F. A., "Natural Convection Across a Vertical Layered Porous Cavity," *International Journal of Heat and Mass Transfer*, Vol. 31, No. 6, 1988, pp. 1247–1260.

[7]Muralidhar, K., Baunchalk, R. A., and Kulacki, F. A., "Natural Convection in a Horizontal Porous Annulus with a Step Distribution in Permeability," *Journal of Heat Transfer*, Vol. 108, No. 4, 1986, pp. 889–893.

[8]Lai, F. C., "Improving Effectiveness of Pipe Insulation by Using Radial Baffles to Suppress Natural Convection," *International Journal of Heat and Mass Transfer*, Vol. 36, No. 4, 1993, pp. 899–906.

[9]Pan, C. P., and Lai, F. C., "Natural Convection in Horizontal Layered Porous Annuli," AIAA Paper 95-0417, Jan. 1995.

Low Prandtl Number Marangoni Convection with a Deforming Interface

Michael R. Mundrane* and Abdelfattah Zebib†
Rutgers University,
Piscataway, New Jersey 08855-0909

Introduction

THERMOCAPILLARY flows are driven by tangential shear associated with temperature-induced surface tension gradients at the interface between two immiscible fluids. In general, this phenomenon continues to generate interest because unsteady convection in crystal growth melts has a negative impact on solid morphology. Unsteady thermocapillary convection calculations for low Pr fluids were performed by Ohnishi and Azuma[1] in a rectangular cavity with an imposed flat-free surface. Their results indicated a transition from steady to unsteady flow at high $Ma \approx 400$, which corresponded to $Re \approx 2.67 \times 10^4$. These results were highly grid dependent in that the critical Ma decreased with each finer grid utilized and were in contrast to steady results calculated by Hadid and Roux[2] where the flow remained steady up to $Ma = 750$. Chen and Hwu[3] performed a numerical solution of both the flowfield and interface for $Pr = 0.01$ and fixed AR $A = 2$. These results indicated a bifurcation at very small Ma and with significant free surface deformation. It was suggested that Ca and critical Ma were inversely related by an exponential relationship and that a flat interface would undergo no transition to unsteady flow. However, Liakopoulos and Brown[4] calculated only steady thermocapillary convection in square cavities with Ca as large as 0.05.

The present work considers thermocapillary convection in a cavity and incorporates a deforming interface using two different approaches. The first is an asymptotic expansion with respect to the small parameter Ca where we develop $\mathcal{O}(1)$ and $\mathcal{O}(Ca)$ solutions. The second approach employs a linearized free surface condition. Details of the formulations are presented with both approaches predicting identical steady states for all parameter values considered.

Mathematical Model

The physical model consists of a rectangular calculation domain with A = width/height. There is a free surface ($y = H$) across which no mass transport takes place. The static contact angle is taken as 90 deg, which implies a flat equilibrium interface. A driving temperature difference ($\Delta T = T_h - T_c$) is imposed in the x direction by assuming differentially heated vertical walls. Adiabatic conditions are assumed at the

Received Nov. 14, 1994; revision received April 18, 1995; accepted for publication April 20, 1995.

*Graduate Assistant, Department of Mechanical and Aerospace Engineering.

†Professor, Department of Mechanical and Aerospace Engineering.

two remaining boundaries. The fluid is Newtonian with velocity components u and v in x and y, respectively. Surface tension σ is assumed to decrease linearly with temperature at a rate γ. Relevant nondimensional parameters are the Prandtl ($Pr = \nu/\alpha$), Reynolds ($Re = \gamma T_r L/\mu\nu$), and Marangoni ($Ma = RePr$) numbers. The symbols ν and μ represent the kinematic and dynamic viscosities, respectively. In addition, the Capillary number ($Ca = \gamma T_r/\sigma_r$) provides some measure of the surface deflection in response to thermocapillary induced stresses. This parameter is small in value and in the limit $Ca \to 0$ (large surface tension), the free surface is flat.

A primitive variable formulation is employed with scales $L = H$, $T_r = T_h - T_c$, $\gamma T_r/\mu$, L^2/ν, and $\gamma T_r/L$ applied to length, temperature, velocity, time, and pressure, which must satisfy

$$\nabla \cdot V = 0 \tag{1}$$

$$V_{,t} + Re\nabla \cdot (VV) = -\nabla p + \nabla^2 V \tag{2}$$

$$T_{,t} + Re\nabla \cdot (VT) = (1/Pr)\nabla^2 T \tag{3}$$

and associated boundary conditions $V = 0$ on $x = 0$, $x = A$, and $y = 0$; $T = 0$ on $x = 0$; $T = 1$ on $x = A$. The interface conditions are[5]

$$(1/Re)h_{,t} + uh_{,x} = v \tag{4}$$

$$(1 - h_{,x}^2)(u_{,y} + v_{,x} + 2h_x(v_{,y} - u_{,x}) = -N(T_{,x} + h_{,x}T_{,y}) \tag{5}$$

$$-P + (2/N^2)[v_{,y} - h_{,x}u_{,y} + h_{,x}(-v_x + h_{,x}u_{,x})] = [(1 - CaT)/Ca](h_{,xx}/N^{-3}) \tag{6}$$

$$h_{,x}T_{,x} - T_{,y} = 0 \tag{7}$$

where $N = (1 + h_{,x}^2)^{1/2}$ and h is free surface deviation from its equilibrium position.

In the first asymptotic approach, the governing equations and boundary conditions are expanded with respect to Ca as $\phi = \phi_0 + \phi_1 Ca + \phi_2 Ca^2 \ldots$. The leading-order problem in Ca is identical to Eqs. (1–3), but with boundary conditions $V_0 = 0$ on $x = 0$, $x = A$, and $y = 0$; $T_0 = 0$ on $x = 0$; $T_0 = 1$ on $x = A$; $u_{0,y} = -T_{0,x}$, $v_0 = 0$, and $T_{0,y} = 0$ on $y = 1$. The $\mathcal{O}(Ca)$ equations and boundary conditions are

$$\nabla \cdot V_1 = 0 \tag{8}$$

$$V_{1,t} + Re\nabla \cdot (V_0 V_1 + V_1 V_0) = -\nabla_{p_1} + \nabla^2 V_1 \tag{9}$$

$$T_{1,t} + Re\nabla \cdot (V_0 T_1 + V_1 T_0) = (1/Pr)\nabla^2 T_1 \tag{10}$$

with $V_1 = 0$ on $x = 0$, $x = A$, and $y = 0$; $T_1 = 0$ on $x = 0$ and $x = A$; and on $y = 1$

$$v_1 = -v_{0,y}h_1 + u_0 h_{1,x} + (1/Re)h_{1,t} \tag{11}$$

$$u_{1,y} = -v_{1,x} - T_{1,x} - (v_{0,xy} + u_{0,yy} + T_{0,xy})h_1 - (2v_{0,y} - 2u_{0,x} + T_{0,y})h_{1,x} \tag{12}$$

$$T_{1,y} = T_{0,x}h_{1,x} - T_{0,yy}h_1 \tag{13}$$

A final compatibility condition on the free surface deformation $h(x, t)$, associated with mass conservation for an incompressible fluid, $\int_0^A h\, dx = 0$, together with free surface boundary conditions $h_1 = 0$ at $x = 0$, A determines h and the arbitrary constant associated with the pressure field: $h_0 = 0$ and $h_{1,xx} = -p_0 + 2v_{0,y}$.

The second approach that assumes $|h| \ll 1$, is to linearize the free surface boundary condition about the equilibrium position. This approach has the advantage that Ca is retained as one of the relevant parameters, but requires a complete solution for each Ca considered. Governing equations are identical to Eqs. (1–3) and the boundary conditions at $y = 1$ are

$$v = (1/Re)h_{,t} + uh_{,x} - v_{,y}h \tag{14}$$

$$u_{,y} = -T_{,x} - v_{,x} - (2v_{,y} - 2u_{,x} + T_{,y})h_{,x} - (v_{,xy} + u_{,yy} + T_{,xy})h \tag{15}$$

$$[(1 - CaT/Ca]h_{,xx} + (u_{,y} + v_{,x})h_{,x} + (p_{,y} - 2v_{,yy})h = -p + 2v_{,y} \tag{16}$$

$$T_{,y} = T_{,x}h_{,x} - T_{,yy}h \tag{17}$$

Nonuniform grids are utilized to increase resolution in regions of higher gradients with each node centered in its respective control volume. Velocities are staggered with central differencing in space. Time marching is accomplished by a fully implicit first-order-forward Euler scheme or by a second-order Crank Nicolson scheme. While the existence of multiple solutions cannot be excluded, the results for a few selected cases using either approach were found to be invariant with respect to a variety of starting conditions. Subsequently, all presented results are obtained using initial conditions consisting of an arbitrary velocity field with a conduction profile. Steady state is declared when maximum relative changes fall below 10^{-9} and remain so for a protracted sequence of time steps, typically larger than 10^5, which correspond to a dimensionless time of 10. The algorithm applied is the semi-implicit method for pressure linked equations, revised (SIMPLER).[6] The present work is performed using a grid dimension of 92×52, which was selected when calculations at this resolution produced results that were within 1 or 2% of those obtained using a 182×102 mesh.

Results

A comparison with available numerical results[4] was performed by prescribing $A = 1$, $Pr = 0.01$, $Ca = 0.05$, $Re = 1000$, and reversing the thermal boundary conditions. The calculated steady flowfield, using either formulation, compares extremely well with that obtained in Ref. 4. The unicellular flow is attracted to the cold corner and the scalar velocity (including maximum obtained value) and surface velocity and deflection profiles are indistinguishable from their figures. Computations with $A = 2$ and $Pr = 0.01$ were performed to allow direct comparison with the results of Chen and Hwu.[3] The obtained flowfields using either formulation are found to be steady for $Re = 2.2 \times 10^2$, 5.0×10^2, 1.0×10^3, or 5.0×10^3. Figures 1 and 2 display both the combined and $\mathcal{O}(Ca)$ flowfields, respectively for $Re = 5.0 \times 10^3$. The combination is performed utilizing an assumed $Ca = 0.01$, which is consistent with the small parameter assumption in the original asymptotic expansion: $\phi \approx \phi_0 + \phi_1 Ca$. The combined and the $\mathcal{O}(1)$ flowfields are indistinguishable for these parameter values.

The flowfield for $Re = 2.2 \times 10^2$ is unicellular with the cell attracted to the cold corner, which is consistent with other work.[7] For this low parameter value, the $\mathcal{O}(1)$ flowfield captures the majority of the flowfield with $\mathcal{O}(Ca)$ corrections limited to the surface and in the vicinity of the cold wall. The flow remains essentially unicellular as Re is increased, but is distorted as a much smaller secondary cell begins to form in the lower hot corner. The contribution of the $\mathcal{O}(Ca)$ correction is primarily in the cold half of the domain or in the immediate vicinity of the free surface for $Re = 2.2 \times 10^2$. As Re is increased, the cold corner, which ultimately dominates the

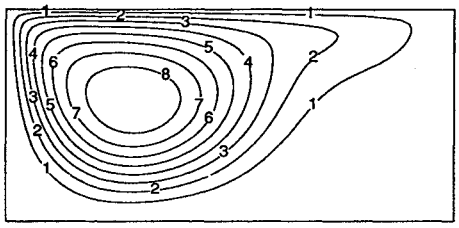

Fig. 1 Combined flowfield for parameter values $A = 2$, $Pr = 0.01$, $Ca = 0.01$, and $Re = 5.0 \times 10^3$. The cold/hot isothermal boundaries are located at $x = 0$, A, respectively. The cold corner dominates the $\mathcal{O}(1)$ flow with increasing Re.

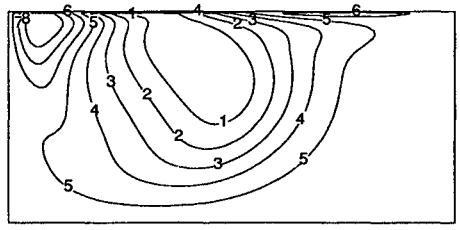

Fig. 2 $\mathcal{O}(Ca)$ flowfield for same parameter values indicated in Fig. 1. This flowfield, which is driven by the $\mathcal{O}(1)$ motion is likewise dominated by the cold corner with increasing Re.

$\mathcal{O}(1)$ flowfield, dominates the $\mathcal{O}(Ca)$ flowfield. However, in contrast to Chen and Hwu,[3] who predict a bifurcation to unsteady flow near $Re = 2.2 \times 10^2$, our results remained steady up through $Re = 5.0 \times 10^3$.

To leading order, the free surface remains flat and, thus, for these results, the free surface distortion exists only as an $\mathcal{O}(Ca)$ correction. The maximum deflection is between 0.3×10^{-3} and 0.5×10^{-3} for the parameter values considered and this small deformation clearly justifies the surface linearization approach for the values of Ca considered here. The interface that we calculated for $Re = 1000$ did not compare well in shape and maximum deflections were several orders of magnitude smaller than that reported in Ref. 3. The dependency of these deflections on A, Pr, and Re can be found elsewhere.[8]

Acknowledgments

We wish to acknowledge the support of NASA through Contract NAG3-1453 and the Pittsburgh Supercomputing Center for computational resources utilized in our work.

References

[1]Ohnishi, M., and Azuma, H., "Computer Simulation of Oscillatory Marangoni Flow," *Acta Astronautica*, Vol. 26, Nos. 8–10, 1992, pp. 685–696.

[2]Hadid, H. B., and Roux, B., "Thermocapillary Convection in Long Horizontal Layers of Low-Prandtl-Number Melts Subject to a Horizontal Temperature Gradient," *Journal of Fluid Mechanics*, Vol. 231, 1990, pp. 77–103.

[3]Chen, J. C., and Hwu, F. S., "Oscillatory Thermocapillary Flow in a Rectangular Cavity," *International Journal of Heat and Mass Transfer*, Vol. 36, No. 15, 1993, pp. 3743–3749.

[4]Liakopoulos, A., and Brown, G. W., "Thermocapillary and Natural Convection in a Square Cavity," *Surface Tension Driven Flows*, edited by G. P. Neitzel and M. K. Smith, Vol. AMD-170, American Society of Mechanical Engineers, New York, 1993, pp. 57–74.

[5]Sen, A. K., and Davis, S. H., "Steady Thermocapillary Flows in Two-Dimensional Slots," *Journal of Fluid Mechanics*, Vol. 121, 1982, pp. 163–182.

[6]Patankar, S. V., *Numerical Heat Transfer and Fluid Flow*, Hemisphere, New York, 1980.

[7]Zebib, A., Homsy, G. M., and Meiburg, E., "High Marangoni Number Convection in a Square Cavity," *Physics of Fluids*, Vol. 28, No. 12, 1985, pp. 3467–3476.

[8]Mundrane, M., Xu, J., and Zebib, A., "Thermocapillary Convection in a Rectangular Cavity with a Deformable Interface," *Advances in Space Research*, Vol. 16, No. 7, 1995, pp. 41–53.

Free Convection in a Horizontal Enclosure Partly Filled with a Porous Medium

D. Naylor*
Ryerson Polytechnic University, Toronto, Ontario MB5 2K3, Canada
and
P. H. Oosthuizen†
Queen's University, Kingston, Ontario K7L 3N6, Canada

Introduction

RECENTLY there has been significant interest in free convection in enclosures partly filled with a saturated porous medium. One of the motivations for studying this problem is the application to the thermal insulation of air spaces. Fibrous and particulate insulating materials can be modeled approximately as a saturated porous medium. In the present numerical study this approach is used to investigate the thermal behavior of a horizontal air gap heated from below, partly filled with a porous insulating material.

Most of the previous studies of free convection in enclosures partly filled with a porous medium have considered vertical enclosures, i.e., vertical heated/cooled walls. For the vertical enclosure, the case of no impermeable barrier between the fluid and porous medium has been studied both numerically and experimentally.[1-3] Tong and Subramanian[4] and Sathe et al.[5] have presented data for a partially filled vertical enclosure with an impermeable barrier between the fluid and porous medium. In these studies it was found that for certain conditions, completely filling an enclosure with a porous medium does not give the minimum convective heat transfer rate. These data suggest that it is possible to optimize the insulation thickness. Hence, the main purpose of the current work is to examine the effect of porous insulation depth on the convective heat transfer rate in a horizontal enclosure heated from below. Partial heating of the lower surface has also been studied as an approximate model of situations involving more localized heat sources, such as hot water pipes routed through an enclosure formed by the structural components of a building.

Problem Formulation and Solution Procedure

As shown in Fig. 1, the present study considers two-dimensional free convection in a square enclosure ($H'/W' = 1$). The central portion of the bottom surface (of length L'_H) is heated to a uniform temperature T'_h and the top of the enclosure is cooled to a uniform temperature T'_c. The enclosure is partly filled with fluid and partly filled with a layer of porous medium (of thickness S'), which is saturated with the

Received Jan. 17, 1995; revision received April 5, 1995; accepted for publication April 6, 1995.

*Assistant Professor, Department of Mechanical Engineering, 350 Victoria Street.

†Professor, Heat Transfer Laboratory, Department of Mechanical Engineering. Member AIAA.